

exploited to construct reporter strains for the rapid screening of novel inhibitors of these critical constituents of the mycobacterial cell wall.

REFERENCES AND NOTES

1. J. B. Bass *et al.*, *Am. J. Respir. Crit. Care Med.* **149**, 1359 (1994).
2. G. Middlebrook, *Am. Rev. Tuberc.* **65**, 765 (1952).
3. K. Johnsson and P. G. Schultz, *J. Am. Chem. Soc.* **116**, 7425 (1994).
4. Y. Zhang, B. Heym, B. Allen, D. Young, S. Cole, *Nature* **358**, 591 (1992).
5. F. G. Winder and P. B. Collins, *J. Gen. Microbiol.* **63**, 41 (1970).
6. F. G. Winder, in *Physiology, Identification, and Classification*, vol. 1 of *The Biology of the Mycobacteria*, C. Rattledge and J. Standford, Eds. (Academic Press, London, 1982), pp. 353-438.
7. L. A. Davidson and K. Takayama, *Antimicrob. Agents Chemother.* **16**, 104 (1979).
8. K. Takayama, E. L. Armstrong, H. L. David, *Am. Rev. Respir. Dis.* **110**, 43 (1974).
9. K. Takayama, L. Wang, H. L. David, *Antimicrob. Agents Chemother.* **2**, 29 (1972).
10. K. Takayama, H. K. Schnoes, E. L. Armstrong, R. W. Boyle, *J. Lipid Res.* **16**, 308 (1975).
11. K. Takayama and L. A. Davidson, in *Mechanism of Action of Antibacterial Agents*, vol. 1 of *Antibiotics*, F. E. Hahn, Ed. (Springer-Verlag, Berlin, 1979), pp. 98-119.
12. B. Heym, P. M. Alzari, N. Honore, S. T. Cole, *Mol. Microbiol.* **15**, 235 (1995).
13. J. M. Musser *et al.*, *J. Infect. Dis.* **173**, 196 (1996).
14. K. Mdluli *et al.*, *ibid.* **174**, 1085 (1996).
15. A. Banerjee *et al.*, *Science* **263**, 227 (1994).
16. J. C. Sacchetti and J. S. Blanchard, *Res. Microbiol.* **147**, 36 (1996).
17. A. Quemard *et al.*, *Biochemistry* **34**, 8235 (1995).
18. S. Morris *et al.*, *J. Infect. Dis.* **171**, 954 (1995).
19. B. Heym *et al.*, *Lancet* **344**, 293 (1994).
20. H. J. Marttila, H. Soini, P. Huovinen, M. K. Viljanen, *Antimicrob. Agents Chemother.* **40**, 2187 (1996).
21. K. L. O'Brien, H. C. Dietz, M. Romahnoli, J. Eiden, *Mol. Cell. Probes* **10**, 1 (1996).
22. K. Mdluli, R. A. Slayden, Y. Zhu, C. E. Barry III, unpublished observations.
23. Single-letter abbreviations for the amino acid residues are as follows: A, Ala; C, Cys; D, Asp; E, Glu; F, Phe; G, Gly; H, His; I, Ile; K, Lys; L, Leu; M, Met; N, Asn; P, Pro; Q, Gln; R, Arg; S, Ser; T, Thr; V, Val; W, Trp; and Y, Tyr.
24. D. J. Prescott and P. R. Vagelos, *Adv. Enzymol.* **36**, 269 (1972).
25. R. G. Summers, A. Ali, B. Shen, W. A. Wessel, C. R. Hutchinson, *Biochemistry* **34**, 9389 (1995).
26. The 10,000g supernatant from a cell lysate of *M. tuberculosis* H37Rv that had been treated with 1 to 5 $\mu\text{g/ml}$ INH was brought to 80% saturation with solid ammonium sulfate. The supernatant from centrifugation at 10,000g was acidified with acetic acid to pH 3.9, centrifuged, and the pellet was redissolved in distilled water. Further purification was accomplished by preparative native gel electrophoresis followed by electroelution.
27. D. Post-Beittenmiller, J. G. Jaworski, J. B. Ohlrogge, *J. Biol. Chem.* **266**, 1858 (1991).
28. We added 10 $\mu\text{g/ml}$ INH for 30 min to 6 liters of mid-log phase *M. tuberculosis* H37Rv in 7H9, ADC, and Tween-80. We then added 7 mCi of [^{35}S]methionine, and after 4 hours, the bacteria were harvested by centrifugation and resuspended in an equal volume of water. This was added to 10 g of 0.1-mm glass beads and homogenized at 4°C for three 1-min pulses by bead-beating and centrifuged at 10,000g for 15 min. The 70 and 80% ammonium sulfate pellets were resuspended in 10 ml of 50 mM sodium phosphate (pH 6.0) containing 0.75 M ammonium sulfate and loaded onto an HP1610 Phenyl-HIC column (Pharmacia). This column was eluted from a concentration of 0.75 M ammonium sulfate until it reached 0 M. Fractions containing the 80-kD protein, determined by protein immunoblot of unlabeled samples, or radioactivity, were combined and dialyzed against 10 mM MES (pH 6.0) before loading onto a Resource Q column equilibrated in the same buffer. After a 2-column volume (CV) wash, the column was eluted over 10 CV to 36% 1 M NaCl in 10 mM MES (pH 6.0) (B), and then to 42% B over another 20 CV, and finally to 100% B over another 10 CV. Appropriate fractions were pooled and concentrated.
29. A. Shevchenko, M. Wilm, O. Vorm, M. Mann, *Anal. Chem.* **68**, 850 (1996).
30. The intact gene cluster was cloned as a Kpn I to Bsp HI fragment into pMV206H (14) which had been cut with Kpn I and Nco I. Transformation of this construct into either *M. smegmatis* or *M. tuberculosis* H37Rv and analysis of the resulting transformants by SDS-polyacrylamide gel electrophoresis (PAGE) showed that none of the encoded proteins appeared significantly up-regulated. *acpM* was cloned individually as an Sph I to Bam HI fragment into pMV261H, and the orientation was determined by restriction mapping. Expression in this construct is driven by the mycobacterial *hsp60* promoter. Transformation of this construct into either *M. smegmatis* or *M. tuberculosis* produced no colonies (<1 colony/ μg of DNA) while transformation of the same gene in the opposite orientation produced between 1×10^3 and 1×10^6 colonies/ μg of DNA. *kasA* was polymerase chain reaction-amplified using *Pwo* polymerase and was cloned into pMH29H, in which transcription is driven by a synthetic mycobacterial promoter sequence. Transformation of this construct into *M. smegmatis* and *M. tuberculosis* produced very small slowly growing colonies. These colonies overproduced KasA protein as demonstrated by SDS-PAGE and protein immunoblotting using affinity-purified antisera to a peptide segment of the KasA primary sequence. It was not possible to accurately assess the INH susceptibility of these colonies because of their impaired growth, but they did not appear to be significantly more resistant to INH than were controls.
31. D. H. Keating, M. R. Carey, J. E. Cronan Jr., *J. Biol. Chem.* **270**, 22229 (1995).
32. DNA was isolated from recent clinical isolates from the collection of J.M.M. HN113 was recovered from the sputum of a patient in Houston, TX, was resistant to INH at >10 $\mu\text{g/ml}$, and had the KatG Ser³¹⁵ \rightarrow Thr³¹⁵ mutation. HN113 had nine copies of IS6110 and belonged to major genetic group 1 (33). Strain HN335 was recovered from a patient in Houston and showed INH resistance at a level of 1 to 2 $\mu\text{g/ml}$. This strain had no mutations in KatG, 14 copies of IS6110, and belonged to group 2. Strain TB029 was recovered from a patient in Japan and was resistant to >10 $\mu\text{g/ml}$ of INH. It contained a KatG Ser³¹⁵ \rightarrow Asn³¹⁵ mutation, four copies of IS6110, and belonged to group 1. Strain HN93 was recovered from a lymph-node biopsy of a Houston patient and showed INH resistance at 1 to 2 $\mu\text{g/ml}$. This strain had a single copy of IS6110 and also belonged to group 1. None of these strains had alterations in the *inhA* locus or upstream of *ahpC*.
33. S. Sreevatsan *et al.*, *Proc. Natl. Acad. Sci. U.S.A.* **94**, 9869 (1997).
34. We thank H. Caldwell for proofreading the manuscript and the NIH-AIDS Research and Reference Reagent Program of NIAID for providing radioactive INH. Supported by USPHS grant AI37004 to J.M.M.

14 January 1998; accepted 12 March 1998

Axonal Swellings and Degeneration in Mice Lacking the Major Proteolipid of Myelin

Ian Griffiths, Matthias Klugmann, Thomas Anderson, Donald Yool, Christine Thomson, Markus H. Schwab, Armin Schneider, Frank Zimmermann, Mailise McCulloch, Nancy Nadon, Klaus-Armin Nave*

Glial cells produce myelin and contribute to axonal morphology in the nervous system. Two myelin membrane proteolipids, PLP and DM20, were shown to be essential for the integrity of myelinated axons. In the absence of PLP-DM20, mice assembled compact myelin sheaths but subsequently developed widespread axonal swellings and degeneration, associated predominantly with small-caliber nerve fibers. Similar swellings were absent in dysmyelinated *shiverer* mice, which lack myelin basic protein (MBP), but recurred in MBP*PLP double mutants. Thus, fiber degeneration, which was probably secondary to impaired axonal transport, could indicate that myelinated axons require local oligodendroglial support.

Proteolipid protein (PLP) is a four-helix-spanning membrane protein thought to stabilize the ultrastructure of central nervous

system (CNS) myelin by forming the double-spaced intraperiod line (IPL), but neither PLP nor its splice isoform DM20 is required for spiral membrane wrapping and myelin compaction (1). Mutations of the X-linked PLP gene (2) cause Pelizaeus-Merzbacher disease (PMD) and spastic paraplegia-2 (SPG-2) in humans and related disorders in animal models, such as the *jumpy* (*jp*) mouse, characterized by premature death of oligodendrocytes and dysmyelination. However, the severe consequences of spontaneous PLP mutations are explained, at least in part, by the toxicity of the encoded

I. Griffiths, T. Anderson, D. Yool, C. Thomson, M. McCulloch, Applied Neurobiology Group, Department of Veterinary Clinical Studies, University of Glasgow, Glasgow G61 1QH, Scotland, UK.

M. Klugmann, M. H. Schwab, A. Schneider, F. Zimmermann, K.-A. Nave, Zentrum für Molekulare Biologie (ZMBH), Universität Heidelberg, Im Neuenheimer Feld 282, D-69120 Heidelberg, Germany.

N. Nadon, Oklahoma Medical Research Foundation, 825 Northeast 13th Street, Oklahoma City, OK 73104, USA.

*To whom correspondence should be addressed. E-mail: nave@sun0.urz.uni-heidelberg.de

polypeptide when misfolded (3).

PLP-DM20-deficient mice containing a null allele develop normally and assemble compacted myelin of appropriate thickness enwrapping small- and large-caliber axons (1). Although the IPL of myelin in these mutants is frequently condensed, oligoden-

drocytes are morphologically normal. Unexpectedly, from the age of 6 to 8 weeks, increasing numbers of focal axonal swellings containing organelles were detected throughout the white and gray matter in all regions of the CNS, particularly in areas where small-diameter myelinated axons pre-

dominate, such as in optic nerves (4). Most spheroids contained numerous dense bodies, multivesicular bodies, and mitochondria (Fig. 1, A and B), often located at the presumptive distal paranode (Fig. 1B). The myelin sheath was preserved over small accumulations of organelles, but became focally

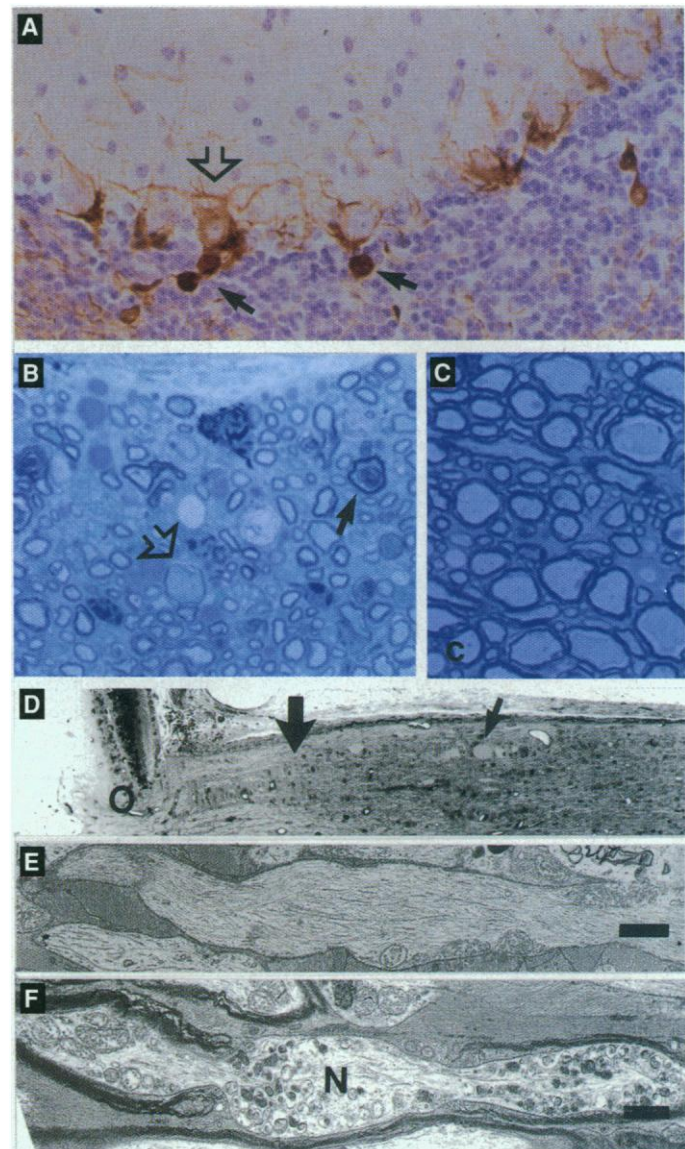
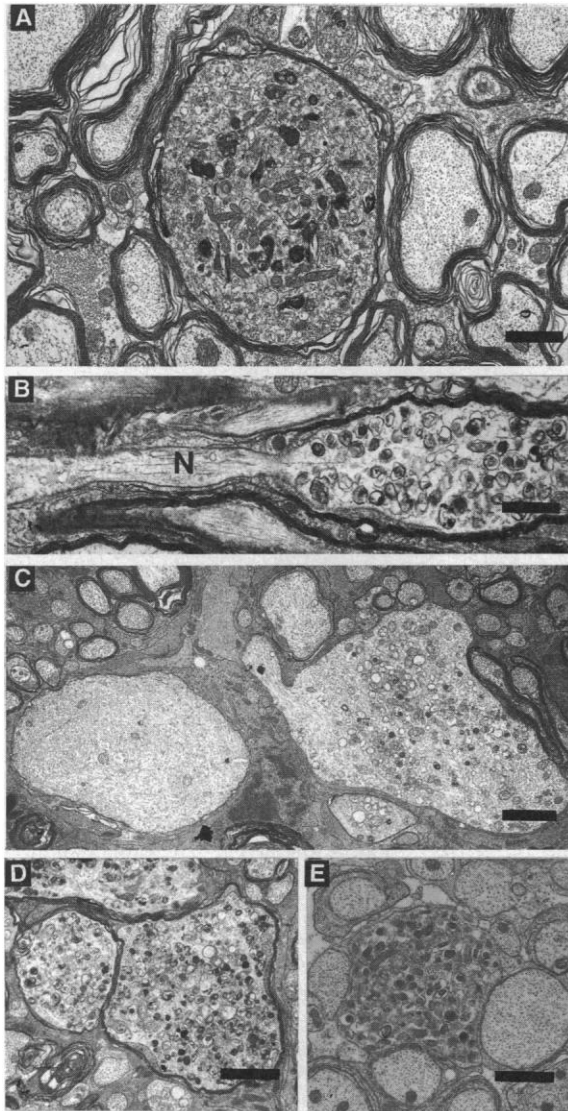


Fig. 1 (left). Axonal spheroids containing membranous organelles in (A) transverse section of the spinal cord and (B) longitudinal section of the optic nerve from a 4-month-old *Plp*^{-/-} mouse. Secondary attenuation of the myelin sheath as a result of slipping is apparent in (A). Axonal swellings often commenced in the paranodal region (B) adjacent to the node of Ranvier (N). (C and D) Large spheroids in the optic nerve of a 1-year-old *Plp*^{-/-} mouse. The swellings in (C) contain predominantly neurofilaments with some organelles, whereas those in (D) contain mainly membranous organelles. As swellings enlarge, the myelin sheath retracts and is eventually lost over the swollen region of the axon [in (C)]. (E) MBP*PLP-deficient double mutants display spheroids identical to those of PLP-deficient mice. All axons are dysmyelinated and many retain an association with ensheathing oligodendrocyte processes. No such swellings were detected in MBP-deficient (*shiverer*) mice. Bars: 1 μ m (A, B, and E); 2 μ m (C and D). **Fig. 2 (right).** (A) Cerebellar cortex from a 4-month-old *Plp*^{-/-} mouse immunostained with antibody RM024 recognizing phosphorylated NF (12) revealing swellings (filled arrows) in Purkinje cell axons. The cell body of one Purkinje cell (open

arrow) contains phosphorylated NFs, suggesting that its axon has degenerated. (B) Degenerating (filled arrow) or swollen (open arrow) small-caliber fibers are apparent in the fasciculus gracilis of a 22-month-old *Plp*^{-/-} mouse. The density of myelinated axons is decreased, indicating axonal loss. In contrast (C), degeneration is not apparent and myelin sheaths are intact in the ventral columns of spinal cord from the same mouse. (D) Proximal region of optic nerve from a 22-month-old *Plp*^{-/-} mouse. Low-power micrograph shows the retina and optic disc (O), the area of the lamina cribrosa (between the retina and the large arrow), and the more distal myelinated region of the nerve (to the right of the large arrow). Some large axonal swellings are visible (small arrow). (E) Unmyelinated axon from lamina cribrosa area of the optic nerve in (D). The axon, surrounded by astrocyte processes, is normal. (F) A myelinated axon at a level just to the right of the large arrow in (D) shows accumulation of organelles at the distal paranode and node (N). The retinal end is to the left. Bars (E and F): 1 μ m.

attenuated and eventually lost through slip-page (5) as swellings enlarged (Fig. 1, C and D). The normal periaxonal space was maintained as predicted by the presence of myelin-associated glycoprotein (1). By 1 year of age, numerous large axonal swellings were present in the optic nerve and spinal cord (Fig. 1, C and D). A smaller proportion of swellings, such as those of Purkinje cell axons ("torpedoes"), were rich in phosphorylated neurofilaments (NFs) (Fig. 2A), but failed to stain with antibodies recognizing dephosphorylated NF epitopes (6). There was no apparent increase in the number of degenerating fibers in the distal compared with the proximal optic nerve, suggesting that the presence of axonal spheroids was not followed immediately by fiber breakdown. At this time, PLP-deficient mice were normal when tested for motor performance on a rotarod (1). In animals older than 1 year, axonal degeneration was more

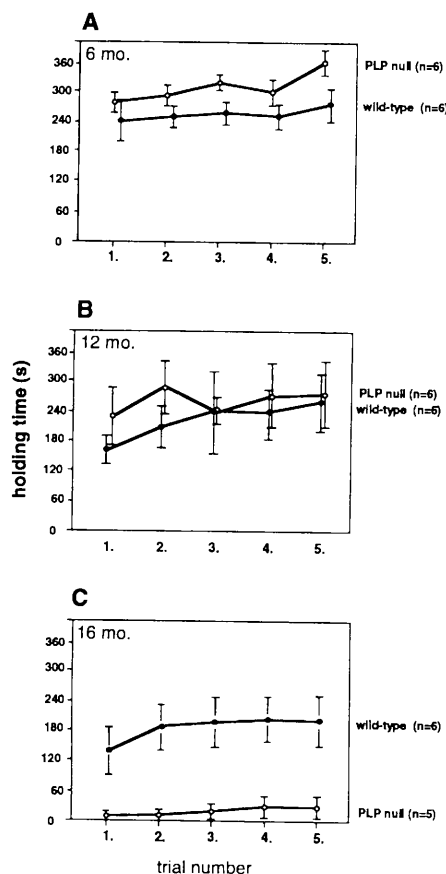


Fig. 3. Loss of motor control in aged PLP-deficient mice. (A to C) A cohort of *Plp*^{-Y} mice (*n* = 6) and age-matched controls of the same sex (*n* = 6) were tested on the rotarod at 6, 12, and 16 months of age (8). The holding time of 16-month-old mutant mice (*n* = 5, one animal died) was decreased compared with WT littermates, which is not apparent at younger ages (1). The motor performance of WT mice was not significantly different between age groups. Error bars are standard deviations.

prominent in the optic nerve and fasciculus gracilis (Fig. 2B), indicating a slow, progressive loss of fibers with age, although neuronal cell loss was not apparent. Increased numbers of microglia and a mild astrocytosis accompanied these degenerative changes (7). Occasional inner-tongue processes of oligodendrocytes contained degenerate organelles. No swellings were detected in wild-type (WT) littermates or in 129/Sv mice, the strain from which the embryonic stem cells were derived.

At older ages, the motor performance of mutant mice appeared altered when the animals' gait was unusually slow and showed signs of spasticity. To quantify these observations, we performed a rotarod test (8) and studied, in a follow-up, a cohort of mutant and WT mice between 6 and 16 months of age. We observed a sudden impairment of motor functions in 16-month-old mice (Fig. 3) without any corresponding evidence of demyelination, for up to at least 22 months (Fig. 2C). Thus, the behavioral phenotype was most likely associated with a threshold effect in the progressive degeneration of CNS axons.

Whereas a null allele of the human PLP gene is associated with a mild peripheral neuropathy (9), our PLP-deficient mice showed no peripheral involvement, even at 22 months of age. Specifically, axons of dorsal root ganglia neurons (which project centrally through the affected fasciculus gracilis) appeared normal. This, and the absence of neurogenic atrophy in skeletal muscle, argues against a major periph-

eral component of the decreased motor performance.

To demonstrate that the absence of proteolipids was the responsible defect, we complemented the mutants (*Plp*^{-Y}) with a WT PLP genomic transgene (10) expressing both PLP and DM20 at nearly normal levels (line tg72). The presence of this transgene completely prevented the axonal pathology in *Plp*^{-Y}*tg72 offspring (Fig. 4). Next, we examined the ability of each isoform, PLP and DM20, to rescue the null mutant. This was achieved by two PLP and DM20 cDNA-based transgenes under control of the human PLP promoter [expressing 70 and 50% of the normal RNA level (11)]. The presence of PLP or DM20 in myelin reduced the axonal changes by 84 and 60%, respectively (Fig. 4), suggesting that both PLP isoforms serve, in principle, the same function.

Myelin-forming glial cells modify axonal morphology (12), but the molecular mechanisms are not known. Schwann cell dysmyelination, caused by mutations of the *Pmp22* and *P0* genes, has also been associated with perturbations of the axonal cytoskeleton and fiber degeneration (13). However, the major changes in myelin volume and composition make it difficult to evaluate the contribution of individual myelin components. This is markedly different in *Plp*^{-Y} mice, in which oligodendrocytes elaborate and maintain appropriately thick myelin sheaths. We examined 4-month-old *shiverer* (*shi*) mice, which lack myelin basic protein (MBP), the second most abundant CNS myelin protein (14). Although the CNS of *shi/shi* mice is poorly myelinated and myelin sheaths lack compaction, no similar spheroids were detected. In contrast, *shi/shi***Plp*^{-Y} double mutants were severely hypomyelinated, but in addition contained the axonal spheroids (Fig. 1E). Thus, axonal swellings appeared to be related to the absence of PLP-DM20 and not to morphologically abnormal myelin.

Because we never observed axonal pathology in normal nonmyelinated fibers, we hypothesized that glial ensheathment provides a necessary signal that induces the axonal dependency on glial support. To distinguish between possible signaling mechanisms that could be either localized (glia to axon) or long-range (glia to neuron), we studied the optic nerve in mouse chimeras. Because of random X chromosome inactivation, both *jp/+* and *Plp*^{+/-} females are mosaics for *Plp* gene expression so that axonal internodes have an equal probability of myelination by WT or mutant oligodendrocytes. In *jp/+* mice, mutant oligodendrocytes fail to myelinate, leaving patches of naked axons (15). In contrast, all optic nerve axons in *Plp*^{+/-} females are normally enwrapped, with about 50% of internodes surrounded by PLP-deficient myelin (1). In adult *Plp*^{+/-} chimeras,

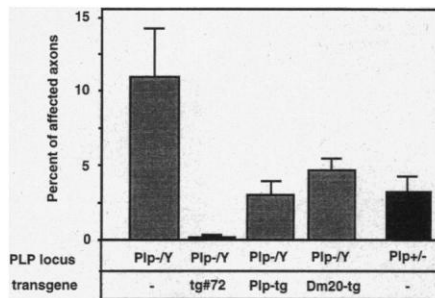


Fig. 4. Quantitation of axonal changes in the optic nerve of PLP/DM20-deficient mice and rescue by transgenic complementation. The combined number of CNS axons, showing abnormal swellings or degeneration, was quantified in cross sections of the mid-optic nerve. In each experiment, the relative proportion of axonal swellings and degeneration profiles was roughly equal (not shown). Complete transgenic complementation was achieved with an autosomal PLP/DM20 genomic transgene (tg72) (10). A partial rescue was observed with both a PLP cDNA (*Plp*-tg) and a DM20 cDNA (*Dm20*-tg) construct, driven by the human PLP promoter (11). Also shown are the changes in female heterozygous mice (*Plp*^{+/-}), whose optic nerves contain a mosaic of PLP⁺ and PLP⁻ myelin sheaths. Each bar represents the mean (\pm SEM) of four mice aged 4 months, with the exception of the heterozygotes (*n* = three mice).

we identified all the morphological signs of axonal swelling and degeneration, although less frequently than in *Plp*-*Y* mice (Fig. 4). Thus, optic nerve axons had become dependent on oligodendrocyte function along their entire length, and WT oligodendrocytes were unable to support adjacent axonal segments enwrapped by PLP-deficient myelin. Oligodendrocytes therefore serve a localized function. In contrast, the nonmyelinated patches of adult *jp/+* mice showed no axonal swellings. Thus, unmyelinated axonal segments of the optic nerve were not oligodendrocyte dependent, a conclusion supported by the absence of swellings in the normally unmyelinated proximal regions in *Plp*-*Y* mice (Fig. 2, D to F). Taken together, the glial-to-axon signaling requires intimate cellular interaction and is also localized. The nature of the signaling molecule is currently unknown, but because PLP-DM20-deficient oligodendrocytes generated this signal after myelination, it cannot be PLP or DM20 itself.

The normal development of myelin in PLP-deficient mice followed by progressive axonal degeneration was unexpected. The axonal defect is best explained if we assume a deficiency of an oligodendroglial function that relates to the maintenance of axonal integrity. The accumulation of membranous dense bodies and mitochondria at distal paranodes strongly suggests an impairment of retrograde axonal transport (16), and the NF swellings may indicate that slow anterograde transport is also compromised, but both will require direct confirmation. It is likely that the complete breakdown of axonal transport at sites of swellings progresses to axonal degeneration before other mechanisms, such as neuronal target deprivation, produce this effect.

Although a supportive function of oligodendrocytes is the most likely explanation of the phenotype under study, two related explanations cannot be formally excluded: (i) The absence of PLP-DM20 from myelin could provide a hostile environment in which axons alter their behavior; (ii) PLP-deficient oligodendrocytes could physically constrict small-caliber axons, although axon "crushes" have never been observed. Indeed, frequency distributions of internodal axonal diameter in optic nerve were normal in 4-month-old *Plp*-*Y* mice (7).

The molecular basis of glial-axonal communication is poorly understood. In invertebrates, a direct vesicular transfer of molecules from glia to axon has been described and may also occur in vertebrates (17). PLP-DM20 is localized in both compact and adaxonal myelin, and the proposed "channel-like" functions of proteolipids (18) could be involved in glial-axonal communication. The lack of connexin-32 from peripheral nervous system myelin underlies a peripheral neuropathy with axonal involvement (19).

The low frequency of axonal spheroids in the few myelinated nerve segments of PLP mutants (20), such as *jimpy*, is probably related to their early death. CNS axonal swellings are also uncommon in adult *rumpshaker* mice (7), presumably because their myelin sheaths incorporate PLP-DM20 (21). The predilection for small-caliber axons is striking; for example, those of the fasciculus gracilis (diameter, $0.96 \pm 0.04 \mu\text{m}$, mean \pm SEM) are affected, but the contiguous larger axons of the fasciculus cuneatus ($2.39 \pm 0.18 \mu\text{m}$) appear, at least morphologically, intact. The reason (or reasons) for the predilection of small-caliber axons is presently unclear.

We suggest a model for neuron-glia interactions in which CNS axons become dependent on oligodendrocyte support some time after myelination has been completed. Accordingly, oligodendrocytes may provide both myelin for rapid impulse conduction and long-term support for axons, a function for which proteolipids and presumably other proteins are required. Whether this function involves the putative channel-like property of PLP (18) awaits further investigation. The principle finding of an oligodendrocyte-dependent axonopathy is relevant to human demyelinating diseases, including multiple sclerosis, where axonal degeneration is now recognized as a major cause of persistent disability (22).

REFERENCES AND NOTES

1. M. Klugmann *et al.*, *Neuron* **18**, 59 (1997); D. Boison and W. W. Stoffel, *Proc. Natl. Acad. Sci. U.S.A.* **91**, 11709 (1994); I. D. Duncan, J. P. Hammang, B. D. Trapp, *ibid.* **84**, 6287 (1987).
2. F. Seitelberger, S. Urbanits, K.-A. Nave, in *Neurodystrophies and Neurolipidoses*, H. W. Moser, Ed. (Elsevier Science, Amsterdam, 1996), pp. 559-579; P. Saugier-Verber *et al.* *Nature Genet.* **6**, 257 (1994); I. R. Griffiths, *BioEssays* **18**, 789 (1996).
3. A. Schneider, C. Readhead, I. Griffiths, K.-A. Nave, *Proc. Natl. Acad. Sci. U.S.A.* **92**, 4447 (1995); A. Gow and R. A. Lazzarini, *Nature Genet.* **13**, 422 (1996); M. Jung, I. Sommer, M. Schachner, K.-A. Nave, *J. Neurosci.* **16**, 7920 (1996).
4. Mice were fixed by intracardiac perfusion of paraformaldehyde-glutaraldehyde or buffered neutral formalin at various ages between 1 day and 22 months. Tissues were prepared for resin or paraffin embedding. Quantification of axonal spheroids and degeneration was performed at the mid-optic nerve of 4-month-old mice by a point-counting method [M. A. Williams, in *Practical Methods in Electron Microscopy*, vol. 6, *Quantitative Methods in Biology*, A. M. Glauert, Ed. (North-Holland, Amsterdam, 1977), pp. 5-84] on electron micrographs at a magnification of $\times 10,000$. About 900 axons per nerve were sampled. Axon diameters in the optic nerve and dorsal funiculus of the cervical spinal cord were measured on the electron micrographs with a digitizer pad and Sumasketch software, sampling ~ 200 axons per region. The proximal or distal orientation of paranodes, relative to the neuronal perikaryon, was made on longitudinal sections of optic nerve, assuming that most fibers were retinofugally directed.
5. R. L. Friede and A. J. Martinez, *Brain Res.* **19**, 165 (1970); R. L. Friede and T. Miyagishi, *Anat. Rec.* **172**, 1 (1972).
6. Paraffin sections were immunostained with peroxidase-antiperoxidase for PLP/DM20 (antibody to COOH-terminal), MBP, and glial fibrillary acidic protein (GFAP, Dako), and for neurofilaments with SMI-31 and SMI-32 (Affiniti Research Products) and with antibodies recognizing phosphorylated and non-phosphorylated NF epitopes (12).
7. I. R. Griffiths, M. Klugmann, K.-A. Nave, data not shown.
8. The rotarod used a motor-driven metal rod with a rough surface (2 cm in diameter, 10 cm wide) flanked by two larger plates. The same cohort of male hemizygous mutant mice ($n = 6$) and age-matched controls ($n = 6$) was analyzed at 6, 12, and 16 months of age. All mice were placed on the roller at rest. After 15 s, the rotarod was started at 1 round per min (rpm). In 60-s intervals, the rotating speed was increased to 2, 4, 8, 12, 16, and 20 rpm. In a series of five consecutive trials per animal, the time (mean \pm SD, in seconds) for which the mice remained on the roller was scored.
9. W. H. Raskind, C. A. Williams, L. D. Hudson, T. D. Bird, *Am. J. Hum. Genet.* **49**, 1355 (1991); J. Y. Garbern *et al.*, *Neuron* **19**, 205 (1997); A. E. Sistermans *et al.*, *Hum. Genet.* **97**, 337 (1996).
10. C. Readhead, A. Schneider, I. Griffiths, K.-A. Nave, *Neuron* **12**, 583 (1994). By appropriate matings, we generated *Plp*-*Y* mice carrying the autosomal PLP transgene. The tg72 transgene was expressed in the CNS of *Plp*-*Y* mice, as revealed by reverse transcriptase-polymerase chain reaction (RT-PCR) and RNA blotting of brain RNA. In situ hybridization and immunostaining (not shown) demonstrated that the expression was confined to oligodendrocytes. Transgenic mutants were hybrids of the mouse strains C57Bl and DBA (in tg72) and 129/Sv (*PLP*-*Y*).
11. N. L. Nadon, H. Arnheiter, L. D. Hudson, *J. Neurochem.* **63**, 822 (1994).
12. B. J. Oldfield and G. M. Bray *J. Neurocytol.* **11**, 627 (1982); I. Sánchez, L. Hassinger, P. A. Paskevich, H. D. Shine, R. A. Nixon, *J. Neurosci.* **16**, 5095 (1996); S. M. De Waegh, V. M. Y. Lee, S. T. Brady, *Cell* **68**, 451 (1992).
13. G. J. Snipes and U. Suter, *Brain Pathol.* **5**, 233 (1995); K. P. Giese, R. Martini, G. Lemke, P. Soriano, M. Schachner, *Cell* **71**, 565 (1992).
14. A. Roach, N. Takahashi, D. Pravtcheva, F. Ruddle, L. Hood, *Cell* **42**, 149 (1985). *shiverer* mice, which have a major deletion of the MBP gene, were mated with *Plp*-*Y* mice to produce double mutants. Mice were genotyped by PCR with genomic DNA from tail biopsies and primer combinations as described (7). Double mutants were hybrids of the mouse strains C3H \times C57Bl (*shi*) and 129/Sv (*PLP*-*Y*).
15. R. P. Skoff and I. N. Montgomery, *Brain Res.* **212**, 175 (1981).
16. R. S. Smith, *J. Neurocytol.* **9**, 39 (1980); S. Tsukita and H. Ishikawa, *J. Cell Biol.* **84**, 513 (1980).
17. T. E. Buchheit and M. Tytell, *J. Neurobiol.* **23**, 217 (1992); M. Tytell, S. G. Greenberg, R. J. Lasek, *Brain Res.* **363**, 161 (1986); A. Duncan, M. Ibrahim, M. Berry, A. M. Butt, *Glia* **17**, 349 (1996).
18. G. Helyncak *et al.*, *Eur. J. Biochem.* **133**, 689 (1983); K. Kitagawa, M. P. Sinoway, C. Yang, R. M. Gould, D. R. Colman, *Neuron* **11**, 433 (1993).
19. J. Bergoffen *et al.*, *Science* **262**, 2039 (1993); P. Anzini *et al.*, *J. Neurosci.* **17**, 4545 (1997).
20. M. P. Dentinger, K. D. Barron, C. K. Csiza, *J. Neurocytol.* **11**, 671 (1982); I. R. Griffiths, I. D. Duncan, M. McCulloch, M. J. Harvey, *J. Neurol. Sci.* **50**, 423 (1981); I. D. Duncan, J. P. Hammang, S. Goda, R. H. Quarles, *Glia* **2**, 148 (1989).
21. A. Schneider *et al.*, *Nature* **358**, 758 (1992).
22. W. I. McDonald, *J. Neuropathol. Exp. Neurol.* **53**, 338 (1994); B. D. Trapp *et al.*, *N. Engl. J. Med.* **338**, 278.
23. We thank H. Krischke and J. M. Barrie for technical assistance and J. Theurer for help with behavioral experiments. We are grateful to N. P. Groome, J.-M. Matthieu, and V. M.-Y. Lee for providing antibodies. This study was supported by Action Research, BBSRC (I.G.), The Wellcome Trust (C.T.), the Oklahoma Center for the Advancement of Science and Technology (N.N.), and by the Deutsche Forschungsgemeinschaft and the European Community Biomed-2 program (K.A.N.).

16 January 1998; accepted 14 April 1998